

CERN-TH/98-222

MRI-PHY/P980756

hep-ph/9807373

Signals of R -Parity Violation at a Muon Collider

Debajyoti Choudhury

*Mehta Research Institute for Mathematics and Mathematical Physics,
Chhatnag Road, Jhusi, Allahabad – 211 019, India.*

Electronic address: debchou@mail.cern.ch

Sreerup Raychaudhuri

Theory Division, CERN, CH 1211 Geneva 23, Switzerland.

Electronic address: sreerup@mail.cern.ch

Abstract

We investigate the effects of R -parity-violating $LL\bar{E}$ and $LQ\bar{D}$ operators on the production of fermion pairs at a $\mu^+\mu^-$ collider with high energy and luminosity. We show that comparison of angular distributions leads to useful discovery limits for the R -parity-violating couplings, especially if the exchanged sfermions turn out to be heavy. Products of these couplings can also be probed well beyond present experimental limits, especially for the second and third generations. Finally, we compare results at a muon collider with those obtainable from an e^+e^- linear collider with similar energy and luminosity.

July 1998

CERN-TH/98-222

1. Introduction

The remarkable success of the Standard Model (SM) of strong and electroweak interactions in explaining a wide range of phenomena at various energies [1] has proved at once a triumph and an embarrassment for high-energy physicists. The triumph is obvious, but the embarrassment is there nevertheless, since the SM is only half-a-theory, having a large number of *ad hoc* assumptions and phenomenological inputs. Moreover, it suffers from a serious theoretical defect — the hierarchy problem — which can only be circumvented by assuming that there is some new physics beyond it at energy scales of a few TeV to a few hundred TeV.

Supersymmetry, allowing the mixture of bosonic with fermionic degrees of freedom, is perhaps the most popular and promising theoretical scenario for physics beyond the SM, as it provides a natural solution for the hierarchy problem. The Minimal Supersymmetric Standard Model (MSSM) [2] is obtained from the SM in a straightforward way by writing down the simplest supersymmetric model that contains the SM as a subset. This involves inclusion of a second Higgs doublet for anomaly cancellation and some soft supersymmetry-breaking terms to account for the fact that no supersymmetric partners of the known SM particles have been discovered (yet), from which it must be inferred that they are heavy. The discovery of supersymmetry will thus require higher energies and luminosities than have been available till the present day. The quest for higher energies has led to several ideas about new colliders and collider techniques, of which one possibility has attracted a great deal of attention: $\mu^+\mu^-$ colliders.

2. Muon Colliders.

Current designs for high-energy colliders make use of beams of electrons, protons or heavy ions. The latter can be accelerated to higher energies, but these energies cannot be tuned in the same way as electron beam energies can. Moreover, QCD backgrounds at hadron colliders are often unmanageably large and render precise measurements difficult. The great advantage of an e^+e^- collider lies in the fact that the final states are relatively clean and free of QCD backgrounds.

The basic motivation for a muon collider stems from the energy and luminosity limitations of e^+e^- colliders. The high luminosities available at the currently running e^+e^- facilities are achieved by having multiple bunch crossings (typically a few thousand) in a storage ring. However, storage rings have a well-known energy limitation due to synchrotron radiation emitted by the rotating electron/positron beams, which has rates in-

versely proportional to the fourth power of the mass of the charged particle. As a result of this, a stage is inevitably reached when all the energy pumped into the electron/positron beam is radiated away. Thus, it seems that the current LEP phase of the CERN Large Electron-Positron (LEP) collider represents the end of the road, as far as e^+e^- storage rings are concerned. To achieve higher energies with electrons, one has to build a *linear* collider, but this naturally leads to a drop in luminosity, as multiple bunch crossings are no longer possible. Various designs for the Next Linear Collider (NLC) are all subject to this disadvantage. The remedy – to have e^- and e^+ sources of extremely high intensity — is obvious, but is expensive and subject to various technical limitations.

Muons represent an interesting alternative to electrons in a storage ring, since they have similar quantum numbers but a mass about 200 times greater than the electron mass — thus reducing synchrotron radiation a billion times. Hence it should be possible to accelerate muons to much higher energies in a storage ring. This is the prime motivation for building a muon collider. At such energies, the muon lifetime increases sufficiently to allow several bunch crossings (typically a few hundred), leading to high design luminosities.

The chief problem in machine design for a muon collider is the fact that the muon, unlike the particles that have been used till now, is an unstable particle, which, despite its increased lifetime at high energies, ultimately tends to decay into an electron and a pair of neutrinos. Thus, as a bunch of muons goes round and round the storage ring, it gradually loses its muon content. Moreover, the electron contamination tends to defocus the beam and introduce a momentum spread, which calls for novel beam-cooling techniques (which are yet to be properly devised). For energies around 300–500 GeV, which have been suggested for the so-called First Muon Collider (FMC), muon decay tends to be a serious limitation to the achievable luminosity. For a higher-energy machine of 2–4 TeV — the Next Muon Collider (NMC) — the muon lifetime increases significantly and much larger luminosities should be achievable. However, beam cooling becomes an even more serious problem here, and until more concrete ideas about the technology become available, it is not clear that a muon machine would be practical and cost-effective. There is also the question of radiation hazards from neutrinos emitted in muon decay: this crosses acceptable safety levels in the neighbourhood of the storage ring at energies of the order of 3 TeV or more.

In view of the technical and financial constraints on building a muon collider, it is important to make a serious study of the physics capabilities of such a machine, especially when compared with a high energy e^+e^- machine such as the NLC. Only if a muon collider can yield substantial improvements over the NLC in the physics output will it be worth investing the time and money required to design and build it. Thus it is important not only to study a muon collider from the point of view of physics capabilities, but also from

a comparative point of view *vis-à-vis* e^+e^- machines.

From the point of view of the physics probed, apart from Higgs-boson Yukawa couplings where the greater mass of the muon plays an important role, the other obvious place to look for differences between a machine with muon beams and one with electron beams is in couplings that differentiate between lepton flavours. Such couplings are absent from the SM but may arise in supersymmetric models in three possible ways, *i.e.* in the soft SUSY-breaking masses of sleptons, in trilinear slepton Higgs boson couplings, and in R -parity-violating couplings, where lepton number is violated. It is the last option that concerns us in this work.

3. R -Parity Violation

Within the perturbative domain of the Standard Model, both baryon number (B) and lepton number (L) are conserved quantum numbers corresponding to global $U(1)$ symmetries. Moreover, there is no leptonic-flavour violation. This, however, is not true for the most general supersymmetric Lagrangian consistent with the $SU(3)_c \times SU(2)_L \times U(1)_Y$ gauge symmetry of the SM. The origin of this can be partly traced to the fact that one of the doublet Higgs superfields (H_1) has the same gauge quantum numbers as the doublet lepton superfields L_i (containing left-handed leptons) and may thus be replaced by any of the latter in the superpotential. Moreover, trilinear terms involving the $SU(2)$ -singlet quark superfields (which incorporate right-handed quarks) are also allowed. The additional pieces in the superpotential may thus be parametrized [3]:

$$\mathcal{W}_R = \mu_i L_i H_2 + \lambda_{ijk} L_i L_j \bar{E}_k + \lambda'_{ijk} L_i Q_j \bar{D}_k + \lambda''_{ijk} \bar{U}_i \bar{D}_j \bar{D}_k, \quad (1)$$

where $\bar{E}_i, \bar{U}_i, \bar{D}_i$ are the singlet superfields and L_i and Q_i are the $SU(2)_L$ -doublet lepton and quark superfields. Although we have dropped $SU(2)_L$ and $SU(3)_c$ indices from the above expression, it is important to note that the coefficients λ''_{ijk} are antisymmetric under the interchange of the last two flavour indices because of the colour symmetry, while the λ_{ijk} are antisymmetric under the interchange of the first two flavour indices because of $SU(2)_L$ invariance.

Of the four terms on the right-hand side of Eq. (1), the first three¹ violate lepton number, while the last violates baryon number. Simultaneous violation of B and L can, however, lead to catastrophically high rates for proton decay. A simple solution is the introduction of a discrete symmetry with a conserved quantum number known as R -

¹The bilinear terms may be rotated away by a redefinition of the fields (L_i, H_1) , with the effect reappearing as λ 's, λ' 's and, possibly, lepton-number-violating soft supersymmetry-breaking terms [4].

parity. Expressible as $R_p \equiv (-1)^{3B+L+2S}$, where S is the intrinsic spin of the particle [5], it cures the problem of rapid proton decay [3] by forbidding *all* the terms in Eq. (1). A particularly interesting consequence of this symmetry is that superpartners of SM particles always appear in pairs at any vertex of the theory and hence the lightest supersymmetric particle (LSP) must be absolutely stable. This has the advantage of providing a possible dark-matter candidate. Moreover, the LSP is expected to interact only weakly with matter, escaping most detectors and leading to rather distinctive missing energy and momentum signatures at high-energy colliders.

Although attractive, the requirement of R -parity invariance is evidently an *ad hoc* one and has no compelling theoretical motivation. Constraints from proton decay can be trivially evaded by demanding, for example, that the theory respects B but not necessarily L . In fact, such an assumption is rather well-motivated within certain theoretical frameworks [7,8], and for the remainder of our article we shall consider B to be a good quantum number of the theory, while L is violated. In fact, vanishing of the λ''_{ijk} couplings renders preservation of GUT-scale baryogenesis [9] much easier than in the case when the couplings are finite. Of course, the presence of the L -violating terms can also affect the baryon asymmetry of the Universe, but the consequent bounds are highly model-dependent and can easily be evaded, for example by conserving just one lepton flavour over cosmological time scales [10].

The last statement draws our attention to the issue of the simultaneous presence of more than one R -parity-violating (R_p) coupling. This usually results in tree-level flavour-changing neutral currents (FCNCs) and hence there exist strong constraints on such scenarios [11], even though *all* products of couplings are not constrained equally. Individual couplings, on the other hand, can be constrained only from low-energy data such as lepton or meson decays [12, 13], neutrino masses [13, 14], neutrinoless double-beta decay [15] and partial widths of the Z -boson [16]. These constraints are neatly summarized in Ref. [17]. As most of these constraints are relatively weak, especially when the mass of the exchanged superparticle is large, they leave enough room for remarkable signals at LEP [14, 18, 19], the Fermilab Tevatron [20] and future colliders. The recent observation of an excess in back-scattered positrons at the DESY HERA collider was initially thought [21] to be just such a signal for R -parity violation, but it now appears more likely to have been a mere statistical fluctuation [22].

In this article, we shall assume that one or at most two of the R -parity-violating couplings are non-vanishing. This is certainly making an assumption, but one can perhaps justify it by pointing at the SM Yukawa couplings where the $t\bar{t}H$ coupling is completely dominant. In any case, most of the effects discussed will not be changed even if a third (or fourth) R -parity-violating coupling is non-zero, though in such a case the low-energy

bounds may be affected.

Under the given assumptions, then, R -parity violation can manifest itself at a muon collider in one of three main ways:

- in pair-production of supersymmetric particles — sfermions or gauginos — mainly through gauge interactions, followed by \mathcal{R}_p decays;
- in resonant production of a supersymmetric particle; and
- in virtual effects in four-fermion processes.

Each of these possibilities requires a detailed analysis. The first possibility would call for an analysis completely analogous to studies at e^+e^- colliders [23] and will not be considered further in this article. In any case, such a study would not be very useful in putting bounds on the \mathcal{R}_p couplings, since most of the results are very weakly dependent on the actual magnitude of these couplings.

To study the other two classes mentioned above, we must examine the consequences of the terms in Eq. (1). In terms of the component fields, we have²

$$\begin{aligned} \mathcal{L}_{\lambda,\lambda'} = & -\lambda_{ijk} \left[\tilde{\nu}_{iL} \overline{\ell_{kR}} \ell_{jL} + \tilde{\ell}_{jL} \overline{\ell_{kR}} \nu_{iL} + \tilde{\ell}_{kR}^* \overline{(\nu_{iL})^c} \ell_{jL} - (i \leftrightarrow j) \right] + \text{H.c.} \\ & -\lambda'_{ijk} \left[\tilde{\nu}_{iL} \overline{d_{kR}} d_{jL} + \tilde{d}_{jL} \overline{d_{kR}} \nu_{iL} + \tilde{d}_{kR}^* \overline{(\nu_{iL})^c} d_{jL} \right. \\ & \left. - \tilde{e}_{iL} \overline{d_{kR}} u_{jL} - \tilde{u}_{jL} \overline{d_{kR}} e_{iL} - \tilde{d}_{kR}^* \overline{(e_{iL})^c} u_{jL} \right] + \text{H.c.} \end{aligned} \quad (2)$$

We first concentrate on the possibility that only one \mathcal{R}_p coupling is non-zero, in which case it is easy to see that no tree-level FCNC effects can be generated. In such a scenario, the most efficient probe is the pair-production of charged fermions, *i.e.* processes of the type:

$$\mu^+ \mu^- \rightarrow f \bar{f} \, , \quad (3)$$

where tagging of the final state is possible if $f = e, \mu, \tau, b$ and (with rather low efficiency) c . It is important to be able to tag the final states because this would enable us to know which of several possible \mathcal{R}_p couplings is involved. Tagging of leptons is rather straightforward, with fairly high efficiencies possible even for taus; tagging of heavy quarks (b, c) is more difficult since it involves observation of displaced vertices; consequently the efficiencies are much lower. It is not possible to tag light-quark flavours; in fact, if the final states involve a pair of light quarks, an excess in dijet final states could certainly be indicative

²We neglect effects due to quark mixing. Such effects could lead to stricter constraints on the couplings [11], but these can then be circumvented in various ways, mostly by allowing some degree of fine tuning.

of some new physics, but it would be difficult to identify the particular R -parity-violating coupling(s) responsible. The possibility of top-quark pair-production needs to be dealt with separately and will not be discussed in this article.

4. Individual \mathcal{R}_p Couplings

The R -parity-violating contribution to four-fermion processes in which the final-state fermions are not muons will come from a t -channel exchange of a sneutrino or a squark, as the case may be. For a $\mu^+\mu^-$ final state, there will be an additional s -channel sneutrino exchange, with the possibility of a resonance (if the sneutrino mass is in the accessible range). In Table 1, we have listed the \mathcal{R}_p couplings that — existing singly — can give rise to four-fermion processes at a muon collider, together with the exchanged sfermion and the final-state particles. We also list there the current experimental bounds [17] on these couplings for a light (heavy) sparticle scenario. The $t\bar{t}$ final states, although they are not considered in this article, are included in the table for the sake of completeness. The upper half of the table is devoted to λ couplings, while the lower half deals with λ' couplings. It is at once apparent that if the single dominant coupling is any one of $\lambda_{131}, \lambda_{133}$ or $\lambda'_{1jk}, \lambda'_{3jk}$, ($j, k = 1, 2, 3$), then it will not contribute to the four-fermion processes under consideration. These couplings cannot, therefore, be measured in isolation at a muon collider. However, the other ones *will* contribute, and may be measured with varying degrees of precision, depending on the final state. The precision will, of course, depend on the efficiency of the tagging algorithm, for which a detailed experimental simulation is required. In the absence of such studies, we have assumed some typical efficiencies for flavour-tagging, which are guided by LEP efficiencies, but are assumed to be uniform over the entire angular range.

The other crucial factor affecting the measurement is the question of backgrounds. It is, of course, immediately obvious that each of these processes will have very large SM backgrounds. The SM contribution arises from γ, Z -mediated s -channel diagrams and, for $f = \mu$, additional t -channel ones too (this process being the muonic analogue of Bhabha scattering). Thus, a measurement of the production rate alone is unlikely to be the most sensitive test for an R -parity-violating contribution. Of course, in the fortuitous case when the machine energy happens to hit on or near a resonance, one can expect a large extra contribution to the cross section for $\mu^+\mu^- \rightarrow \mu^+\mu^-$. This can, then, lead to rather good measurements of the sneutrino mass and the responsible R -parity-violating coupling [27]. However, one must also allow for the possibility that the sparticle resonance lies beyond the energy reach of the muon collider and hence only virtual effects will be observable. These represent smaller deviations from the SM cross sections, and, as such,

require a more sensitive test to isolate from the background.

Coupling	Final state	Exchange	Channel(s)	Upper bound
λ_{121}	e^+e^-	$\tilde{\nu}_e$	t	0.05 (0.5)
λ_{122}	e^+e^-	$\tilde{\nu}_\mu$	t	0.05 (0.5)
	$\mu^+\mu^-$	$\tilde{\nu}_e$	$s+t$	
λ_{123}	$\tau^+\tau^-$	$\tilde{\nu}_e$	t	0.05 (0.5)
λ_{131}	—	—	—	
λ_{132}	e^+e^-	$\tilde{\nu}_\tau$	t	0.06 (0.6)
	$\tau^+\tau^-$	$\tilde{\nu}_e$	t	
λ_{133}	—	—	—	
λ_{231}	e^+e^-	$\tilde{\nu}_\tau$	t	0.06 (0.6)
λ_{232}	$\mu^+\mu^-$	$\tilde{\nu}_\tau$	$s+t$	0.06 (0.6)
	$\tau^+\tau^-$	$\tilde{\nu}_\mu$	t	
λ_{233}	$\tau^+\tau^-$	$\tilde{\nu}_\tau$	t	0.06 (0.6)
λ'_{1jk}	—	—	—	
λ'_{211}	$d\bar{d}$	\tilde{u}_L	t	0.09 (0.9)
	$u\bar{u}$	\tilde{d}_R	t	
λ'_{212}	$s\bar{s}$	\tilde{u}_L	t	0.09 (0.9)
	$u\bar{u}$	\tilde{s}_R	t	
λ'_{213}	$b\bar{b}$	\tilde{u}_L	t	0.09 (0.9)
	$u\bar{u}$	\tilde{b}_R	t	
λ'_{221}	$d\bar{d}$	\tilde{c}_L	t	0.18 (1.8)
	$c\bar{c}$	\tilde{d}_R	t	
λ'_{222}	$s\bar{s}$	\tilde{c}_L	t	0.18 (1.8)
	$c\bar{c}$	\tilde{s}_R	t	
λ'_{223}	$b\bar{b}$	\tilde{c}_L	t	0.18 (1.8)
	$c\bar{c}$	\tilde{b}_R	t	
λ'_{231}	$d\bar{d}$	\tilde{t}_L	t	0.22 (2.2)
	$t\bar{t}$	\tilde{d}_R	t	
λ'_{232}	$s\bar{s}$	\tilde{t}_L	t	0.39 (3.5)
	$t\bar{t}$	\tilde{s}_R	t	
λ'_{233}	$b\bar{b}$	\tilde{t}_L	t	0.39 (3.5)
	$t\bar{t}$	\tilde{b}_R	t	
λ'_{3jk}	—	—	—	

Table 1. *List of R-parity-violating couplings and four-fermion processes to which a single dominant coupling can contribute. The exchanged sparticle is shown, together with the current experimental bound. The numbers shown correspond to the case when the exchanged sparticle (relevant to the bound) has a mass of 100 GeV (1 TeV) and the perturbative limit $\sqrt{4\pi} \sim 3.5$ if there is no bound. If the couplings do not lead to four-fermion processes at a muon collider, the bounds (even where they exist) are not listed.*

Whatever the situation may be, and especially if the latter case should turn out to be true, it is often more useful to consider the differential cross sections for four-fermion

processes rather than the overall rates. A comparison of the experimentally measured angular distributions of leptons or jets with those predicted in the SM might give a hint of the presence of \mathcal{R}_p contributions that are lost in the integrated cross sections. For all the processes, except those leading to a $\mu^+\mu^-$ final state, the \mathcal{R}_p contribution arises in the t -channel, whereas the SM background arises from s -channel processes. Thus, one would expect a strong forward peak in the \mathcal{R}_p contribution, which is absent from the SM background. For the $\mu^+\mu^-$ final states, both signal and background will have both t - and s -channel sfermion exchanges, so that the difference in angular distribution may not prove so striking, but here the s -channel resonance is likely to yield large excess contributions to the new physics effect, even when the machine energy is not exactly tuned to the resonance.

In order to obtain a measure of the angular distribution, we integrate the differential cross section over the scattering angle in bins of 5° each for leptonic final states and 10° each for hadronic final states. Of course, in practice, hadronic jets would extend over several bins, but we assume that the jet direction — as determined by its thrust axis — can be determined to a precision of $\pm 5^\circ$. This assumption enables us to make a parton-level Monte Carlo analysis of the problem. A more refined analysis is certainly required at a later stage, but should not make qualitative changes in the results shown here.

The number N_i of events predicted in a bin i (assuming a given \mathcal{R}_p coupling and a sneutrino mass) is obtained by multiplying the integrated cross section in that bin by the machine (integrated) luminosity \mathcal{L} and the detection efficiency $\epsilon_{f\bar{f}}$ for the particular fermion pair under consideration,

$$N_i = \epsilon_{f\bar{f}} \mathcal{L} \sigma_i . \quad (4)$$

We then calculate the corresponding number N_i^0 in the SM for each bin and use the two sets of numbers to construct the variance

$$\chi^2 = \sum_i^{\text{bins}} \left(\frac{N_i - N_i^0}{\Delta N_i^0} \right)^2 . \quad (5)$$

The error ΔN_i^0 in Eq. (5) is obtained by adding the statistical error and a projected systematic error δN_i^0 in quadrature:

$$\Delta N_i^0 = \sqrt{(\sqrt{N_i^0})^2 + (\delta N_i^0)^2} . \quad (6)$$

This systematic error is a theoretician's apology for an experimental analysis and we take it to be 2% for all the bins, *i.e.* $\frac{\delta N_i^0}{N_i^0} = 0.02$. Of course, the actual figure may be somewhat different from this and will probably vary over different bins. However, we include it as a

zeroth-order estimate. Obviously χ^2 grows as the mismatch between the two distributions grows and can be taken as a measure of the new-physics effect.

To be quantitative, we adopt the energy and luminosity parameters given by the Accelerator Physics Study Group at the Fermilab Workshop on the First Muon Collider [28]. For the FMC, these are

$$\begin{aligned}\sqrt{s} &= 350, 500 \text{ GeV}; \\ \mathcal{L} &= 10 \text{ fb}^{-1},\end{aligned}\tag{7}$$

which we shall denote FMC-350 and FMC-500 respectively. For the NMC these parameters are

$$\begin{aligned}\sqrt{s} &= 2, 4 \text{ TeV}; \\ \mathcal{L} &= 10^3 \text{ fb}^{-1},\end{aligned}\tag{8}$$

which we shall denote NMC-2 and NMC-4 respectively.

Accurate flavour tagging demands that the outgoing leptons or jets in Eq. (3) be at least 20° away from the beam pipe. This is indicated by preliminary studies [28] of the electron contamination in the initial muon beam. Within this restricted region, we now assume uniform detection efficiencies [29]

$$\epsilon_{ee} = \epsilon_{\mu\mu} = 0.9, \quad \epsilon_{\tau\tau} = 0.8, \quad \epsilon_{b\bar{b}} = 0.3, \quad \epsilon_{c\bar{c}} = 0.1.\tag{9}$$

These are again *ad hoc* assumptions (albeit guided by LEP efficiencies), but they cannot really be improved until the detector is actually designed.

Dividing the angular region between 20° and 160° into equal-sized bins of $5^\circ(10^\circ)$ each for leptonic (hadronic) final states leads to 28 (14) bins. To avoid spurious contributions to the variance χ^2 we drop a bin from the sum in Eq. (5) if either (i) the difference between the SM expectation and the measured number of events is less than 1 or (ii) the SM expectation is less than 1 event. However, the high luminosities ensure that this does not affect the numerical results significantly. We then present the discovery limits from such an analysis in the form of 95% C.L. contours in the space of the sfermion mass and the \mathcal{R}_p coupling. A signal will be deemed observable if the χ^2 of Eq. (5) exceeds the minimum acceptable fluctuation [30] for 28 (14) random variables. Before we discuss our results, a few observations are in order.

- Throughout our analysis, we shall assume that only one sfermion (and its isospin partner, if any) is ‘light’. In other words, that the left-chiral and right-chiral sfermions have widely different masses. Hence we shall not combine limits from processes with differing sfermion propagators.

- Although it might seem inappropriate to consider four-fermion processes mediated by sfermions that are light enough to be pair-produced, it is not quite so. For, even in the case of a pair of sfermions being produced, a determination of the strength of possible \mathcal{R}_p interactions from a study of the branching fractions is likely to be very difficult. The four-fermion mode can then play a complementary role in pinning down the actual value of the \mathcal{R}_p coupling.
- All our results for dijet final states are based on a parton-level analysis. While jet fragmentation details may affect the results somewhat, the qualitative features will remain unchanged.
- We neglect all initial-state radiation (ISR) effects. This, of course, is a much better approximation for a muon collider than for an e^+e^- one. Some small changes may occur, though probably not enough to change the qualitative features of our work. However, if it is proposed to tune a muon collider to a sneutrino resonance (assuming it has previously been discovered), then ISR effects could be critical.
- In an actual experimental study, one must demand that the energies of the final lepton or jet pair match the beam energy well. This would serve to remove both ISR effects and backgrounds from SM (or MSSM) processes where one or more particles escape undetected.

Once all these caveats and approximations are taken into account, Fig. 1 shows the discovery limits for the λ couplings, obtainable by studying dilepton states, while Figs. 2 and 3 show the discovery limits for the λ' couplings, obtainable by studying dijet states. In view of the large number of curves in each figure, and the different possibilities for \mathcal{R}_p couplings, these cases merit separate discussion.

Dilepton final states:

In Fig. 1(a), we illustrate the limits achievable from $\mu^+\mu^- \rightarrow \mu^+\mu^-$ for the relevant couplings (see Table 1) λ_{122} and λ_{232} with $\tilde{\nu}_e$ and $\tilde{\nu}_\tau$, respectively, being exchanged in both s and t channels. The current low-energy bounds on these are shown by (solid) parallel straight lines in the figure, the upper one denoting λ_{232} and the lower one denoting λ_{122} . The dashed line shows the reach in the λ - $M_{\tilde{\nu}}$ plane for the coupling λ_{122} at LEP (λ_{232} cannot be measured in isolation at an e^+e^- collider) running at a centre-of-mass energy of 190 GeV and accumulating 300 pb^{-1} of data, the last being a fairly conservative assumption for the LEP collider when the data of all four experiments are combined. Of course, for the LEP bounds on the λ_{122} coupling, one needs to study³ the t -channel

³See also Section 6, where the case of e^+e^- colliders is discussed at length.

sneutrino exchange process $e^+e^- \rightarrow \mu^+\mu^-$. Solid lines show the discovery reach at the FMC-350 and FMC-500, and at the NMC-2 and NMC-4.

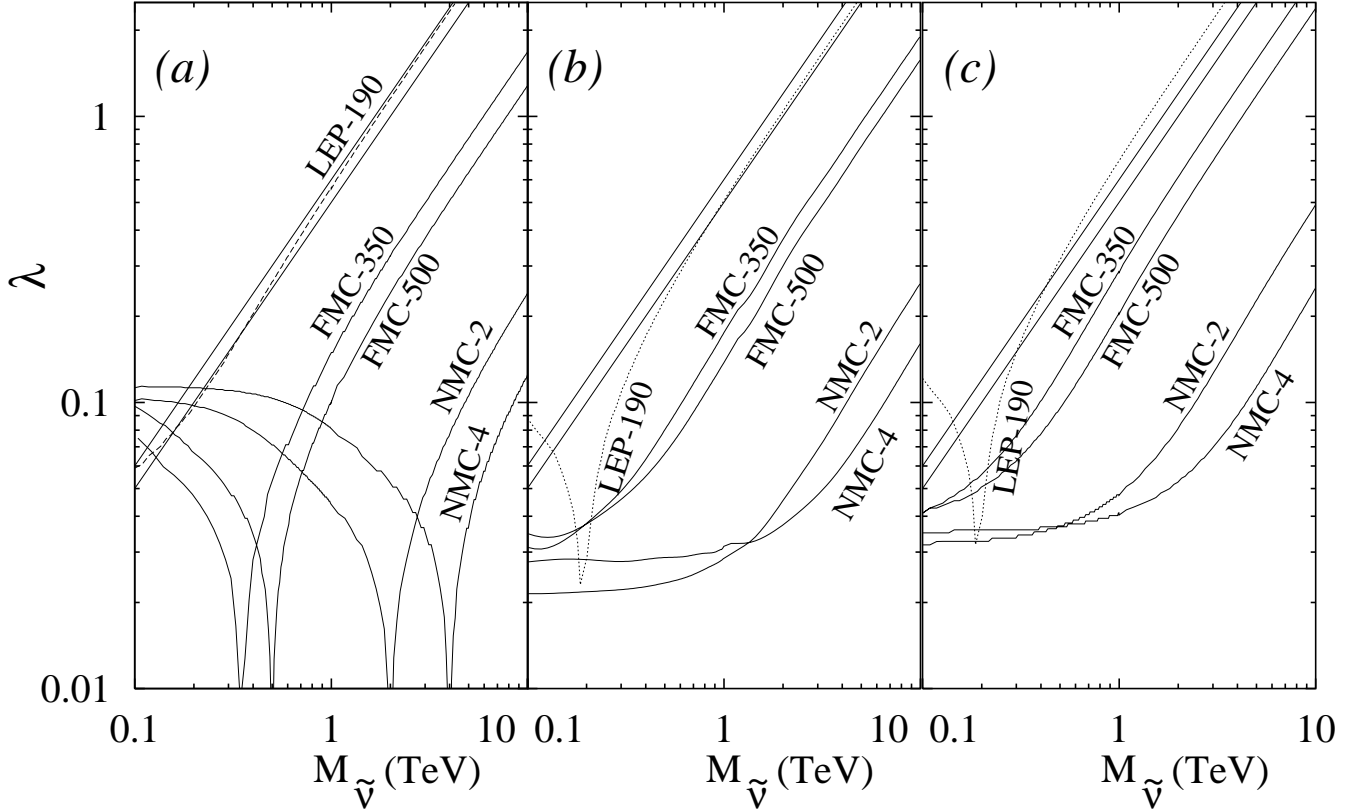


Figure 1: *Illustrating the reach at a muon collider in the \mathcal{R}_p parameter space ($LL\bar{E}$) when (a) the differential cross section for a $\mu^+\mu^-$ final state is considered, (b) the differential cross section for an e^+e^- final state is considered, and (c) the total cross sections for an e^+e^- final state are considered. The part of the parameter space above the curves can be excluded at 95% C.L. The oblique straight lines correspond to low-energy bounds on the relevant couplings (see text).*

The sharp dips in the contours correspond to the resonance production of a sneutrino that subsequently decays into $\mu^+\mu^-$ through the same coupling. As mentioned above, the large cross section at the resonance enables us to probe much smaller values of the coupling than when the sneutrino is an off-shell one. For the purposes of this graph, the sneutrino width is taken to be 200 MeV. Such a value assumes that the sneutrino decays almost exclusively through \mathcal{R}_p channels, which may not always be true, since it is possible for the sneutrino to decay to lepton–gaugino final states. This assumption automatically restricts us to the part of the MSSM parameter space where gauginos are heavier than the sneutrino. A complementary study by Feng, Gunion and Han [27] discusses the situation when the gauginos are light.

Fig. 1(a) makes it clear that it should be possible, at a muon collider, to place rather

stringent bounds⁴ on the couplings λ_{122} and λ_{232} , which go far beyond what can be inferred from low-energy data or from the data expected in the current run of LEP. In fact, it is obvious that LEP can barely improve upon the low-energy bound on λ_{122} , even when the sneutrino mass is 1 TeV or more. The situation is clearly more promising at a muon collider, especially when the sneutrino mass exceeds 200 GeV. Much of this is due to resonance effects. In fact, near the peak, bounds on λ_{122} and λ_{232} can be improved by a whole order of magnitude. Even away from the resonance, if a muon collider is built and runs in all the above modes, one can rule out values of $\lambda > 0.06$ all the way up to a sneutrino mass of 5–6 TeV.

The situation is somewhat different when a resonance is absent, as Fig. 1(b) and 1(c) demonstrate. Fig. 1(b) shows the discovery limits for an e^+e^- final state, which implies one of the couplings λ_{121} , λ_{122} , λ_{132} or λ_{231} . Once again, the oblique straight lines demarcate the region ruled out by low-energy data; the lower line is relevant for λ_{121} , λ_{122} and the upper one for λ_{132} , λ_{231} . The dashed line shows the bounds available from LEP on λ_{121} , which can cause a sneutrino resonance in Bhabha scattering at LEP (see Section 6). We see that muon colliders could again do better than the low-energy data, especially in the higher sneutrino mass region. For the λ_{122} coupling, a combination of Fig. 1(a) and (b) can reduce the bound to about 0.015 for sneutrino masses upto a few TeV. It is interesting that one gets, in general, better bounds from the non-resonant case of e^+e^- final states than can be obtained from the case of $\mu^+\mu^-$ final states (unless, indeed, the machine energy happens to hit on a sneutrino resonance in the latter case). This is because of the extra t -channel diagrams in the SM background for the $\mu^+\mu^-$ final state, which make the signal and background look rather similar, as far as angular distributions go.

To illustrate the usefulness of comparing differential cross sections, in Fig. 1(c) we have shown the discovery limits obtainable from a consideration of the total Bhabha cross section for $\mu^+\mu^- \rightarrow e^+e^-$. We simply calculate the fluctuation in the total SM cross section by a formula identical to Eq. (6) (assuming a 2% systematic error) and require the excess supersymmetric contribution to exceed this at 95% C.L. As before, dashed lines show the bounds available from LEP, from a consideration of the total cross section only. It is immediately obvious that comparison of differential cross sections by the method of Fig. 1(b) leads to better discovery limits than a consideration of the total cross section. In fact, with the latter approach, the LEP bounds would hardly better the low-energy bounds (unless a resonance is hit upon), and though the FMC could improve these, it will cover less of the parameter space than that shown in Fig. 1(b). The NMC, of course, does pretty well in either case, simply by virtue of its high energy and luminosity, but again,

⁴In this and the subsequent discussions, we refer to an improvement of bounds, but it is, of course, possible that a discovery may be made.

this method fares somewhat worse than that of Fig. 1(b).

Both Figs. 1(a) and 1(b) show a crossover between the two lines representing the FMC discovery limits. A similar phenomenon occurs for the NMC. This implies that, for lower values of sneutrino mass, it is actually more efficient to have a lower-energy machine than a higher-energy one (with the same luminosity). This apparent paradox is actually an artefact of the cuts. For higher energies, the sneutrino mass becomes progressively negligible, and thus the excess contribution, being driven by a t -channel exchange, is more and more peaked at small angles. Since precisely this part of the distribution is rendered inaccessible by detector limitations, the relative excess is reduced at higher energies.

An analysis of the $\tau^+\tau^-$ final state results in very similar plots for the couplings λ_{123} , λ_{132} , λ_{232} or λ_{233} (the last two are inaccessible at LEP). The small differences reflect the fact that, at a muon collider, tau-tagging efficiency is expected to be close to that for tagging muons (SEe Eq. (9)). We, therefore, choose not to present these plots. It must be remembered, however, that for the λ_{123} and λ_{132} couplings at LEP, a t -channel sneutrino exchange is relevant and hence we need to replace the dotted curve of Fig. 1(b) with the dashed curve of Fig. 1(a).

Dijet final states:

We now turn to the possibility of dijet final states, where effects due to λ' couplings could manifest themselves. These are qualitatively similar to the $\mu^+\mu^- \rightarrow e^+e^-$ case, since the new-physics effect arises from the replacement of a t -channel sneutrino by a t -channel squark. There are quantitative differences, however. One is the obvious fact that the cross sections are changed because of the colour factor and the different weak quantum numbers of quarks. A greater difference arises because tagging efficiencies for heavy b, c quarks are low and the lighter flavours cannot be tagged at all. Without tagging, we can tell very little about which individual coupling is responsible for the excess events, if they are seen. Of course, if no deviation is seen, *all* the couplings that could have resulted in such an excess are automatically bounded, but the converse is certainly not true.

Perhaps it would not be out of place to explain how the tagging efficiency affects the χ^2 fitting of the distribution. It is apparent from Eqs. (4) and (5) that decreased efficiency decreases the effective luminosity and thus increases the relative statistical error in Eq. (5). As a result, it becomes more difficult to differentiate the signal from the background through a χ^2 analysis. Another issue of great importance in the study of dijets is the question of charge identification. Using the wisdom of LEP estimates and practice, we assume that charge identification is possible for heavy quark jets and that it may or may not be possible for light-quark jets. If charge identification is possible, then the scattering angle θ is uniquely defined and may be treated in the manner described above, dividing

the range $20^\circ < \theta < 160^\circ$ into 14 bins of 10° each. However, if charge identification is not possible, then it will not be possible to distinguish between θ and $\pi - \theta$; hence one should add to the cross section in the bin $20^\circ < \theta < 30^\circ$ the cross section in the bin $150^\circ < \theta < 160^\circ$, and so on. Thus, we get a total of 7 bins, with a corresponding dilution of the capacity to distinguish between signal and background. However, the minimum χ^2 requirement is also reduced, so there is a partial trade-off between the two effects, as we shall see presently.

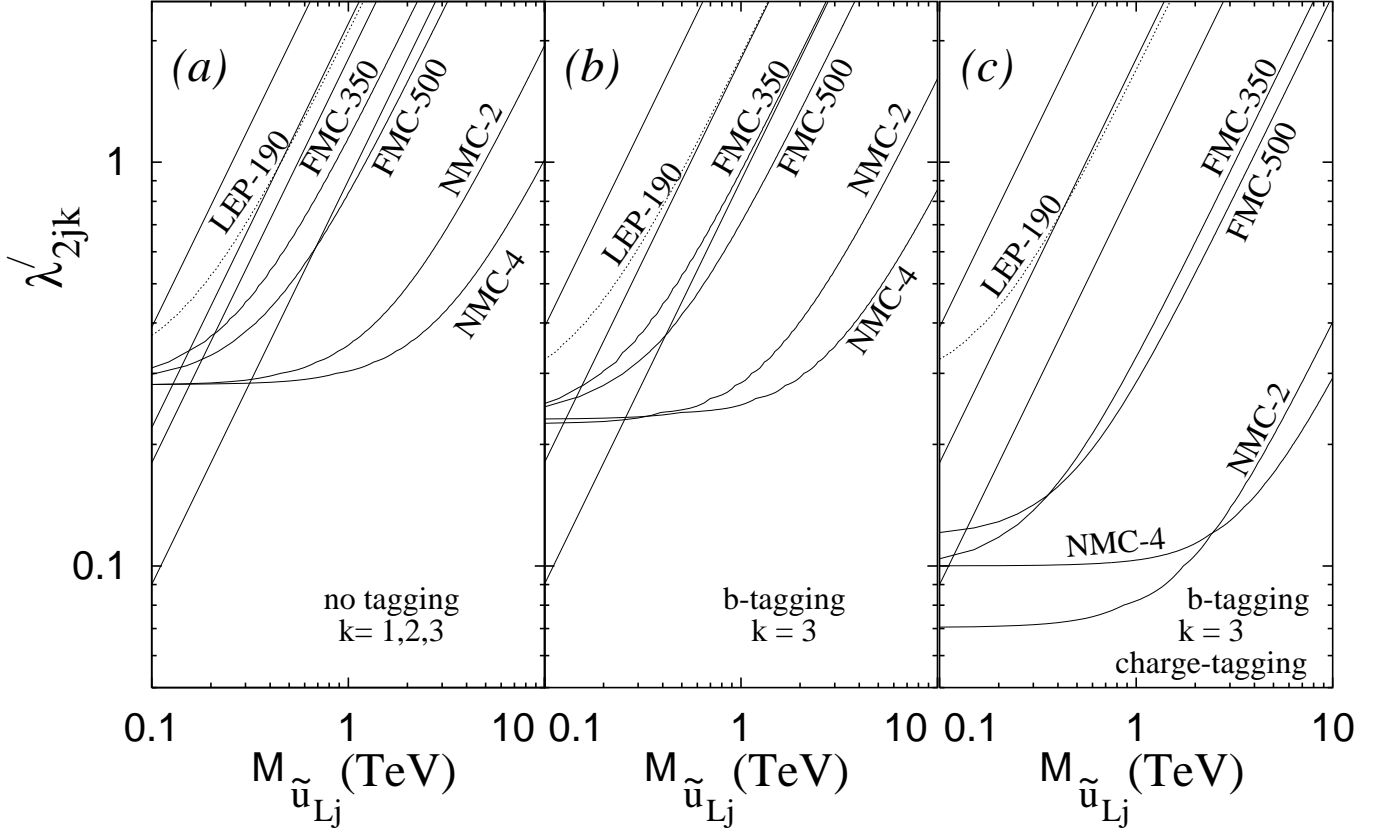


Figure 2: Illustrating the reach of a muon collider in the \mathcal{R}_p parameter space ($LQ\bar{D}$), assuming exchange of a \tilde{u}_L -type squark, when (a) the differential cross section for an untagged dijet final state is considered, (b) the differential cross section for a tagged $b\bar{b}$ final state is considered, but we assume no charge identification, and (c) the differential cross section for a tagged $b\bar{b}$ final state is considered, assuming charge identification with unit efficiency. The oblique straight lines correspond to low-energy bounds on the relevant couplings (see text).

In Fig. 2(a), we show the discovery limits obtainable for the λ'_{2jk} ($j, k = 1, 2, 3$) couplings from a consideration of dijet final states, where no attempt is made to tag the jets. For this figure, we assume that the exchanged squark has charge $\frac{2}{3}$ and hence the excess will appear in $d\bar{d}$, $s\bar{s}$ or $b\bar{b}$ states. Of course, *all* the light quarks, irrespective of charge, will form part of the SM background. Naturally, there is no resonance involved here and hence the curves look rather like those in Fig. 1(b). The difference lies in the

different coupling, the fact that we use a broader binning for hadronic jets and the fact that there is no charge identification. Most important, however, is the sheer magnitude of the SM background, to which all light quarks contribute. All of the λ' couplings listed in Table 1 can contribute to this figure, and hence the bounds from this are the most general of all. The dotted line shows possible LEP bounds, but it should be remembered that these correspond to a different set of couplings λ'_{1jk} . As in Fig. 1, the four oblique (solid) lines show the low-energy bounds on the λ'_{2jk} couplings, which may be read off from Table 1. We have not shown the bounds on the λ'_{1jk} , which are rather more tight than those on the λ'_{2jk} (so that the figure is slightly misleading as regards the LEP bounds), but these may be readily found in Ref. [17]. Thus the figure tells us that a muon collider can probe $\lambda'_{2jk} \gtrsim 0.25$ for $M_{\tilde{\nu}} \lesssim 1$ TeV.

In Fig. 2(b), we show the discovery limits obtainable from a consideration of $b\bar{b}$ final states, where both the b -jets are tagged, but charge identification is not done. The bounds are valid for the couplings λ'_{2j3} , ($j = 1, 2, 3$), as a glance at Table 1 will show. The three straight lines in the top left-hand corner denote (in ascending order), the bounds on λ'_{2j3} , where $j = 1, 2, 3$ respectively, and the dotted line shows what LEP can achieve for the couplings λ'_{1j3} , given 300 pb^{-1} of data. Again, the graphs resemble those of Fig. 1(b), for reasons explained above; but it is clear that the low tagging efficiency for b -jets compared with that for electrons or positrons leads to less striking results at the FMC. At the NMC, the high luminosity comes to the rescue, since the smallest difference in cross section now gets magnified in the construction of χ^2 . It is also interesting that even with the rather low (~ 0.3) efficiency of tagging b -jet pairs, there is a significant difference between the accessible region with and without b -tagging. This may be attributed to a large decrease in the background with the removal of other quark flavours leading to dijets. A much more striking improvement occurs once charge-identification is assumed. This is illustrated in Fig. 2(c), where it is further assumed that the charge of the tagged b -jets can be identified with 100% efficiency. Why is this so. To understand this feature, we must examine the angular distribution of the b -jet, which is peaked in the forward hemisphere. On the other hand, the *relative* deviation due to a small \mathcal{R}_p coupling is more pronounced in the backward hemisphere, although the cross sections are considerably smaller. In the absence of charge identification, since θ is indistinguishable from $\pi - \theta$, we need to sum over the paired bins and the relative deviation is thereby reduced⁵. This, in turn, reduces the contribution to the χ^2 , and thus the sensitivity to λ' .

In Fig. 3(a), we again show the discovery limits obtainable on the couplings λ'_{2jk} ,

⁵A numerical example will help clarify this. For a certain choice of parameters, the SM prediction for the bin $40^\circ\text{--}50^\circ$ is 80 events, with 85 events for the \mathcal{R}_p case. The same choice leads to 12 SM events in the bin $130^\circ\text{--}140^\circ$, with 16 events for the \mathcal{R}_p case. We thus get $\chi^2 = 0.303 + 1.327 = 1.63$ for the case when both bins are considered, and $\chi^2 = 0.849$ when they are merged into a single bin.

($j, k = 1, 2, 3$) from a consideration of dijet final states, where no attempt is made to tag the jets. For this figure, we assume that the exchanged squark has charge $-\frac{1}{3}$ and hence the excess will appear in $u\bar{u}$ or $c\bar{c}$ states. As before, all the light quarks, irrespective of charge, will form part of the SM background. The graph differs from Fig. 2(a) only in that the interference terms between the \tilde{R}_p -contribution and the SM ones lead to a larger excess cross section because of the different quantum number assignments of the final states. For this reason, the bounds could be significantly better. In fact, we could then probe $\lambda'_{2jk} \gtrsim 0.1$ all the way up to $M_{\tilde{\nu}} \simeq 1$ TeV.

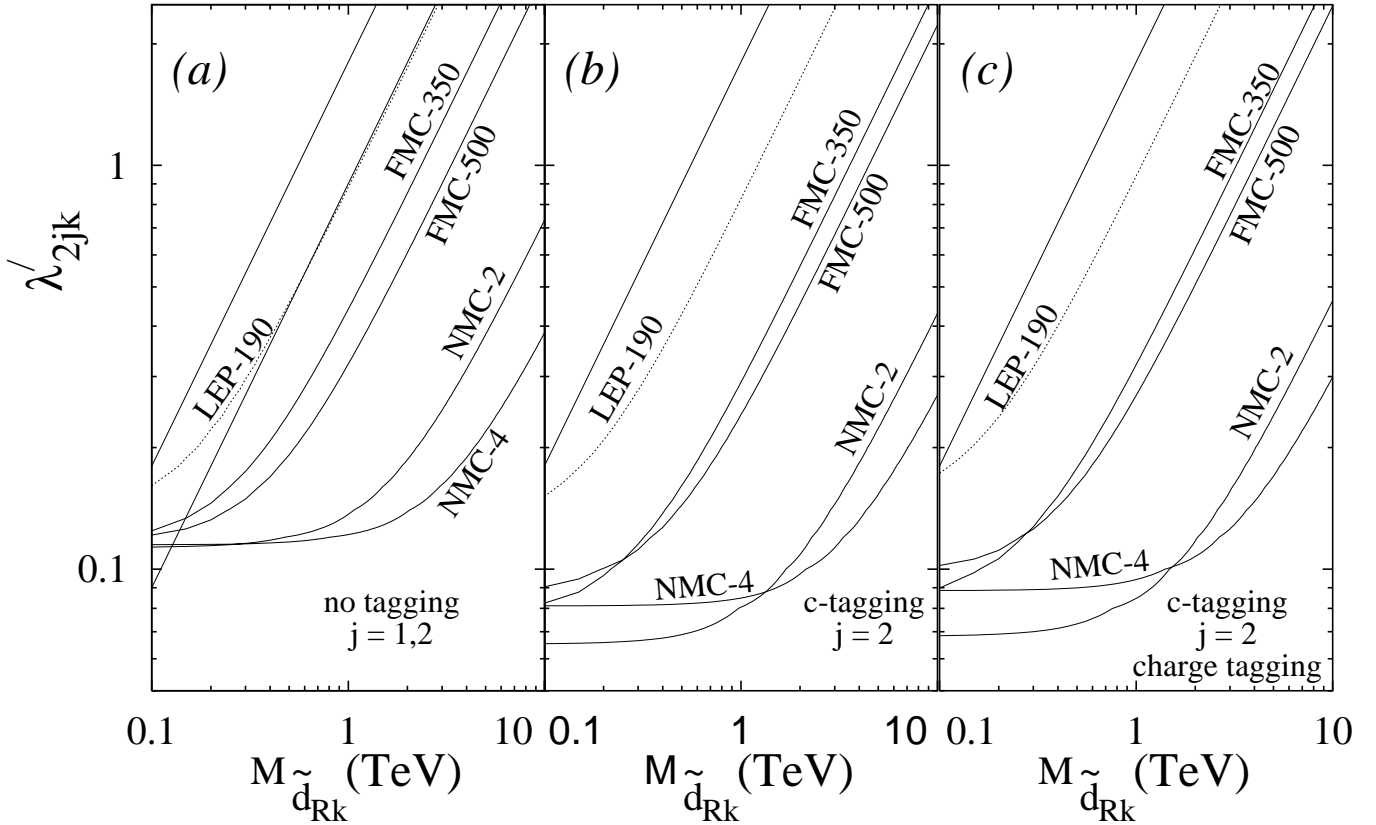


Figure 3: As in Fig. 2, but assuming exchange of a \tilde{d} -type squark, and tagged $c\bar{c}$ final states.

In Fig. 3(b), as in Fig. 2(b), we show the discovery limits obtainable from a consideration of $c\bar{c}$ final states, where both jets are tagged as arising from c -quarks, but charge identification is not attempted. This means the couplings involved must be λ'_{22k} , ($k = 1, 2, 3$) (see Table 1). Here the bounds are actually stronger than in the case of b -jets, despite the efficiency for tagging c -quarks being rather poor (~ 0.1). This is because the excess cross section for charge $\frac{2}{3}$ final states is larger than that for charge $-\frac{1}{3}$ ones, essentially on account of large interference terms that are strongly dependent on the quantum-number assignments of the final-state quarks. Rather surprisingly, given the arguments presented above for the case of $b\bar{b}$ final states, not much improvement is achieved by identifying

the charge of the parent c -quarks (Fig. 3(c)). This paradox is simply resolved by noting that, for the case of u -type quarks, the difference between signal and background is more pronounced in the forward hemisphere, where the cross section is larger. Thus the major contribution to the χ^2 comes from the forward hemisphere and separating out the backward hemisphere has little effect on the result. What little improvement is attained is, in fact, washed out by the requirement of a larger χ^2 when we double the number of bins. Thus, it might be useful to simply look at the seven bins in the forward hemisphere. For $c\bar{c}$ final states, then, unlike the $b\bar{b}$ case, charge identification is not a major issue.

We conclude this section with the remark that a comparison of Fig. 1 with Figs. 2 and 3 shows that high tagging efficiency does not necessarily imply a better reach in the space of R -parity-violating couplings. This reach depends on several features, and the quantum numbers of the final-state fermions play a crucial role in its determination.

5. Products of \mathcal{R}_p Couplings

We next consider the possibility that more than one of the couplings in Eq. (1) is non-zero. This situation is rather more complicated. Clearly, one interesting possibility is to have tree-level FCNCs, which would then be susceptible to various bounds from low-energy processes. Many of these have been studied and various bounds may be found in the literature [11]. In a muon collider, FCNC interactions will manifest themselves in several ways, the simplest being in processes such as $\mu^+\mu^- \rightarrow f_i\bar{f}_j$ ($i \neq j$), where i and j label different flavours. Experimentally, such mixed-flavour final states are easiest to detect when f_i, f_j are charged leptons. In this case, the final state will be indicative of a product of two couplings both of the λ type, with an exchanged sneutrino. There will be virtually no SM background for these processes and very small backgrounds (if at all) from other supersymmetric processes involving lepton flavour-mixing (since these occur at the one-loop level) [24]. Thus, one can simply search for unlike-flavour lepton pairs as a signal for R -parity-violating scenarios where more than one coupling is non-zero.

The recent results from Super-Kamiokande [25], indicating the occurrence of neutrino oscillations, may perhaps be thought to lead to mixing of charged lepton states as well, within the framework of the SM itself. However, even if such mixings occur, the effects must be so small as to have evaded detection (to date) in all low-energy experiments. The size of the detector is, of course, much too small to see oscillations between charged leptons. Thus, such effects would be negligible at a muon collider and would not interfere with any signals due to \mathcal{R}_p -interactions.

Product Λ^2	Final state	Exchange	Channel(s)	UpperBound
$\lambda_{121}\lambda_{122}$	$e\mu$	$\tilde{\nu}_e$	$s + t$	$6.6 \times 10^{-7(5)}$
$\lambda_{121}\lambda_{123}$	$e\tau$	$\tilde{\nu}_e$	t	$5.6 \times 10^{-3(1)}$
$\lambda_{122}\lambda_{123}$	$\mu\tau$	$\tilde{\nu}_e$	$s + t$	$5.7 \times 10^{-3(1)}$
$\lambda_{122}\lambda_{131}$	$e\tau$	$\tilde{\nu}_e$	s	$6.7 \times 10^{-3(1)}$
$\lambda_{122}\lambda_{132}$	$\mu\tau$	$\tilde{\nu}_e$	$s + t$	$6.4 \times 10^{-3(1)}$
$\lambda_{122}\lambda_{133}$	$\tau\tau$	$\tilde{\nu}_e$	s	—
$\lambda_{131}\lambda_{232}$	ee	$\tilde{\nu}_\tau$	s	—
$\lambda_{132}\lambda_{232}$	$e\mu$	$\tilde{\nu}_\tau$	$s + t$	—
$\lambda_{133}\lambda_{232}$	$e\tau$	$\tilde{\nu}_\tau$	s	$5.6 \times 10^{-3(1)}$
$\lambda_{231}\lambda_{232}$	$e\mu$	$\tilde{\nu}_\tau$	$s + t$	—
$\lambda_{231}\lambda_{233}$	$e\tau$	$\tilde{\nu}_\tau$	t	$6.7 \times 10^{-3(1)}$
$\lambda_{232}\lambda_{233}$	$\mu\tau$	$\tilde{\nu}_\tau$	$s + t$	$6.4 \times 10^{-3(1)}$
$\lambda_{i22}\lambda'_{i11}, \lambda_{i22}\lambda'_{i22}$	dijet	$\tilde{\nu}_i$	s	—
$\lambda_{i22}\lambda'_{i21}, \lambda_{i22}\lambda'_{i12}$	dijet	$\tilde{\nu}_i$	s	$3.8 \times 10^{-7(5)}$
$\lambda_{i22}\lambda'_{i13}, \lambda_{i22}\lambda'_{i23}$	dijet (one b)	$\tilde{\nu}_i$	s	—
$\lambda_{i22}\lambda'_{i33}$	$b\bar{b}$	$\tilde{\nu}_i$	s	—
$\lambda'_{2i1}\lambda'_{2i2}$	dijet	\tilde{u}_{iL}	t	$3.8 \times 10^{-7(5)}$
$\lambda'_{2i1}\lambda'_{2i3}, \lambda'_{2i2}\lambda'_{2i3}$	dijet (one b)	\tilde{u}_{iL}	t	—
$\lambda'_{21i}\lambda'_{22i}$	dijet (one c)	\tilde{d}_{iR}	t	—
$\lambda'_{21i}\lambda'_{23i}$	≤ 4 jets (one b)	\tilde{d}_{iR}	t	—
$\lambda'_{22i}\lambda'_{23i}$	≤ 4 jets (one b , one c)	\tilde{d}_{iR}	t	—

Table 2. List of products of R -parity-violating couplings that can be measured in four-fermion processes at a muon collider. The exchanged sparticle is shown, together with the current experimental bounds, applicable in the case of a sparticle mass \tilde{m}^2 of 100 GeV. The bounds scale as \tilde{m}^2 . Dashes in the last column signify that no non-trivial bounds obtain from low-energy FCNC processes.

Another equally interesting possibility to see products of pairs of λ couplings is to have sneutrino resonances in $\mu^+\mu^- \rightarrow e^+e^-$ or $\tau^+\tau^-$. These will also arise from two different λ -type couplings involving the same sneutrino. For these signals, the SM background is large and it is again better to look at the differential cross sections rather than the total rates, and use the same isolation technique as for a single coupling. However, if it is possible to tune the energy exactly to the mass of the resonance, then one can certainly achieve very high accuracy in the measurement [27]. Some of these products of λ couplings could also lead to unlike-flavour final states in s -channel processes. If both s - and t -channel processes are allowed, bounds on the relevant products would closely resemble those on single couplings arising in $\mu^+\mu^- \rightarrow \mu^+\mu^-$. Finally, an exciting possibility arises when we consider $e\tau$ final states, since these can receive contributions from the products $\lambda_{122}\lambda_{131}, \lambda_{232}\lambda_{133}$ and may help us to measure the couplings $\lambda_{131}, \lambda_{133}$, which are not

measurable in isolation at a muon collider.

In the upper half of Table 2, we have listed the possible products of pairs of dissimilar λ couplings that could be accessible at a muon collider, together with the exchanged sparticle and the current experimental bounds. Only 12 out of 36 possible products can be accessed⁶. As in Table 1, the (low-energy) bounds assume that the mass of the exchanged sparticle is 100 GeV, with numbers in parentheses for the same bounds when the exchanged sparticle has a mass of 1 TeV.

Following the convention set up in Table 1, the lower half of Table 2 lists possible products of pairs of λ' couplings that might be investigated at a muon collider. Measuring these would require improved tagging efficiencies, with the best chances being for $b\bar{q}$ final states. As in Table 1, we have listed four-jet states arising from the production of single top quarks [26] for the sake of completeness, but we have not studied these states in this article.

It is also possible to investigate products of one λ -type coupling with another one of the λ' type. In this case, the λ coupling appears in the coupling of a sneutrino resonance to a muon–antimuon pair, while the λ' coupling appears at the other end, where a pair of quarks is produced. For products of the form $\lambda_{i22}\lambda'_{i33}$, one has the interesting possibility of a (sneutrino) resonance contribution to scalar Higgs production at a muon collider (which is not really surprising, since sneutrinos have the same quantum numbers as Higgs bosons and can, in fact, mix with them if lepton number is not conserved). This possibility has been studied in Ref. [27] and will not be discussed further in this article.

In Fig. 4, we show the accessible part of the parameter space for the cases when the final state consists of a fermion pair, and all tagging efficiencies have been set to unity. The three cases correspond to exchange of a sneutrino in (a) the s -channel, with the possibility of large resonance contributions, (b) the t -channel and (c) both s - and t -channels, with smaller effects due to resonances. As in Fig. 1, the dotted lines correspond to bounds from LEP (on a different set of products, given in Table 4). We have not shown the low-energy bounds on the products as there are too many of them; however, they are listed in Table 2. To generate this figure, we have assumed that a point in the parameter space is accessible if 5 or more dissimilar fermion pairs are generated in 10 fb^{-1} of data. This criterion appears reasonable for leptons, but a larger number may be necessary for jets. Of course, the curves will then simply scale as the square root of that number. One must also scale the curves suitably by the relevant tagging efficiencies. For example, for an $e\tau$ state, we need to scale up the curves by $\sqrt{\epsilon_{e\tau}}$ where $\epsilon_{e\tau} = \sqrt{\epsilon_{ee}\epsilon_{\tau\tau}} \simeq 0.85$. It is hardly necessary to point out that better bounds can be obtained when there is a t -channel exchange of

⁶The remaining 24 can be found in Table 4.

a light sneutrino, since s -channel amplitudes suffer a natural suppression because of the high energy of the FMC and the NMC (unless a resonance is hit).

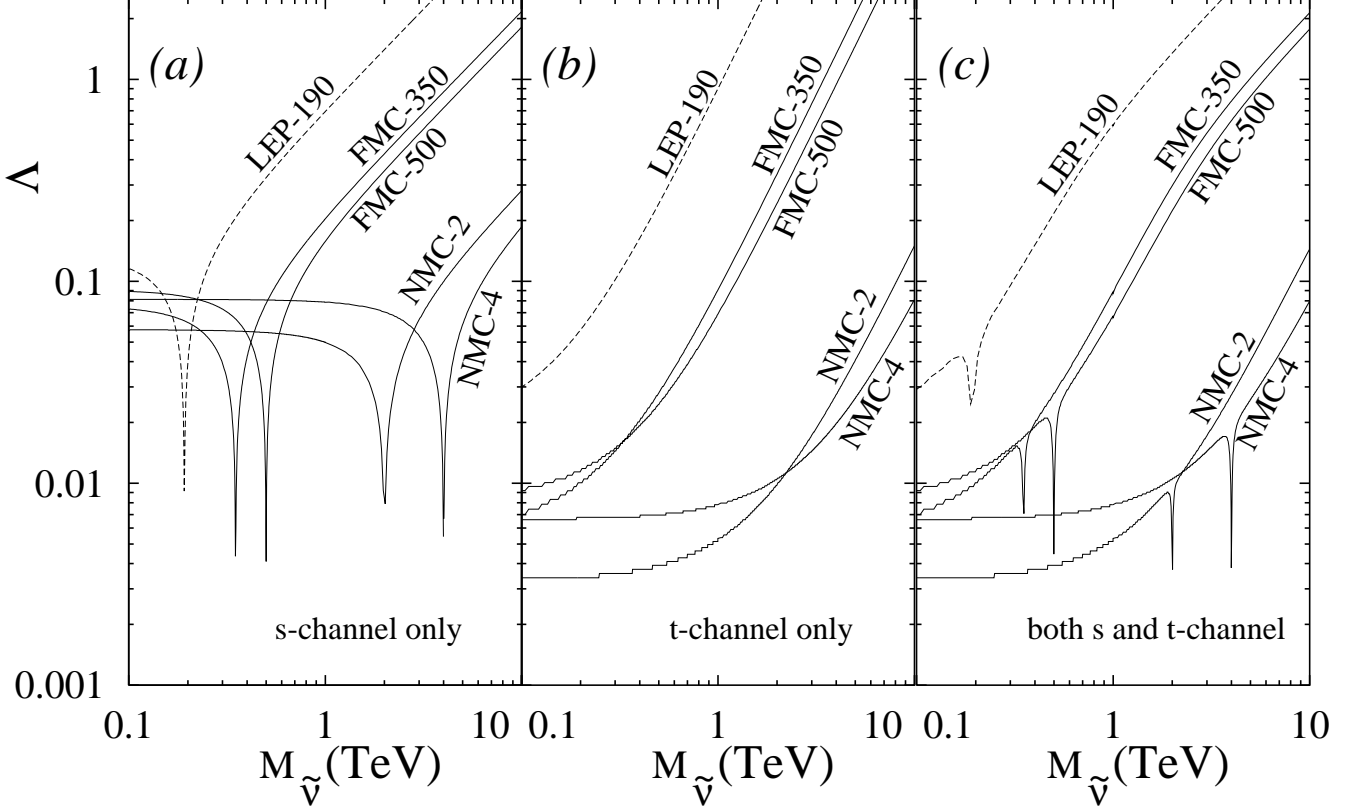


Figure 4: Illustrating the reach of a muon collider in the R_p parameter space for products Λ of pairs of couplings when (a) an s -channel sneutrino exchange is considered, (b) a t -channel sneutrino exchange is considered, and (c) both s - and t -channel exchanges are considered. Dotted lines showing the LEP bounds correspond to products different from those accessible at a muon collider: they are only included for comparison. All tagging efficiencies are set to unity.

For products of λ' couplings, the exchanged particle will be a squark, but the actual bounds will be very weak, since the number of excess events will either be multiplied by the low b and c tagging efficiencies, or, if one looks at untagged dijets, the excess must be greater than the 95% C.L. fluctuation in the expectation for the SM dijet production. The actual numbers for the latter, given the parameters chosen for this work, are about 196 for LEP, 1223 and 629 for the FMC at 350 GeV and 500 GeV respectively, and 3268 and 911 for the NMC at 2 TeV and 4 TeV respectively. These large values make it clear that it will not be possible to probe small values of R_p couplings. We do not consider a study of products of two λ' couplings worth its while and shall not mention them any further in this article.

6. Comparison with an e^+e^- Collider

As explained in Section 2, the major motivation for building a muon collider is the limited energy and luminosity of an e^+e^- machine. However, it is very likely that a 350–500 GeV linear e^+e^- collider will, in fact, be built. This is the so-called Next Linear Collider (NLC), for which several plans exist. Such a machine will probably have an integrated luminosity of about 10 fb^{-1} , which makes it completely competitive with the FMC, though falling short of both the energy and luminosity of the NMC. Hence, as explained in Section 2, it is necessary to compare our results at a muon collider with similar predictions at the NLC. The physics analysis (within our assumptions and approximations) is rather similar in the two cases. Even the angular cut of 20° around the beam pipe, which is imposed in the case of a muon collider, will be required at the NLC to avoid beamstrahlung effects. Thus there is some justification in using the numerical results we have obtained for the FMC to make predictions for the NLC as well.

Final state	Coupling at $\mu^+\mu^-$	Exchange at $\mu^+\mu^-$	Coupling at e^+e^-	Exchange at e^+e^-
e^+e^-	λ_{121}	$\tilde{\nu}_e(t)$	λ_{121}	$\tilde{\nu}_\mu(s+t)$
	λ_{122}	$\tilde{\nu}_\mu(t)$	$*\lambda_{131}$	$\tilde{\nu}_\tau(s+t)$
	λ_{132}	$\tilde{\nu}_\tau(t)$		
	λ_{231}	$\tilde{\nu}_\tau(t)$		
$\mu^+\mu^-$	λ_{122}	$\tilde{\nu}_e(s+t)$	λ_{121}	$\tilde{\nu}_e(t)$
	λ_{232}	$\tilde{\nu}_\tau(s+t)$	λ_{122}	$\tilde{\nu}_\mu(t)$
			λ_{132}	$\tilde{\nu}_\tau(t)$
			λ_{231}	$\tilde{\nu}_\tau(t)$
$\tau^+\tau^-$	λ_{123}	$\tilde{\nu}_e(t)$	λ_{123}	$\tilde{\nu}_\mu(t)$
	λ_{132}	$\tilde{\nu}_\tau(t)$	λ_{131}	$\tilde{\nu}_e(t)$
	$*\lambda_{232}$	$\tilde{\nu}_\mu(t)$	$*\lambda_{133}$	$\tilde{\nu}_\tau(t)$
	$*\lambda_{233}$	$\tilde{\nu}_\tau(t)$	λ_{231}	$\tilde{\nu}_\mu(t)$

Table 3. Comparison between a $\mu^+\mu^-$ and an e^+e^- collider for processes leading to bounds on individual \mathcal{R}_p couplings of the $LL\bar{E}$ type. An asterisk (*) indicates that the coupling is measurable at only one of the two kinds of collider.

The chief difference between an e^+e^- collider and a $\mu^+\mu^-$ collider lies in the different flavour of the initial state, which means that the same final state will produce bounds on an R -parity-violating coupling with *different* flavour indices. To keep track of these, we list in Table 3 the accessible couplings for the same final state at both e^+e^- and $\mu^+\mu^-$ colliders. We also mention (in parentheses) whether an s - or a t -channel resonance is responsible for the excess events predicted, which enables one to identify the relevant plots in Figs. 1, 2 and 3. For example, for a single \mathcal{R}_p coupling and an $s+t$ -channel exchange, one must take the dashed (LEP) curve from Fig. 1(b) and the solid (FMC)

curves from Fig. 1(a). For t -channel exchanges, we need the dashed curve from Fig. 1(a) and the solid curves from Fig. 1(b).

What immediately stands out from Table 3 is the fact that the results from a $\mu^+\mu^-$ machine nicely *complement* those obtainable at an e^+e^- collider. The two couplings, λ_{232} and λ_{233} , which are not accessible at an e^+e^- collider, are accessible at a muon collider. On the other hand, the muon collider cannot measure λ_{131} and λ_{133} , which an e^+e^- collider can. Clearly it would be useful to have both sets of measurements. For the five couplings that can be measured at both machines, the same complementarity holds. For example, λ_{121} is measurable at either machine, but it can be better measured at a muon collider

Serial No.	Product Λ^2	F.S. at $\mu^+\mu^-$	Exchange at $\mu^+\mu^-$	F.S. at e^+e^-	Exchange at e^+e^-
1	$\lambda_{121}\lambda_{122}$	$e\mu$	$\tilde{\nu}_e(s+t)$	$e\mu$	$\tilde{\nu}_\mu(s+t)$
2	$\lambda_{121}\lambda_{123}$	$e\tau$	$\tilde{\nu}_e(t)$	$e\tau$	$\tilde{\nu}_\mu(s+t)$
3, 4, 5	$\lambda_{121}\lambda_{13k}$	—	—	—	—
6	$\lambda_{121}\lambda_{231}$	—	—	$e\tau$	$\tilde{\nu}_\mu(s)$
7	$\lambda_{121}\lambda_{232}$	—	—	$\mu\tau$	$\tilde{\nu}_\mu(s)$
8	$\lambda_{121}\lambda_{233}$	—	—	$\tau\tau$	$\tilde{\nu}_\mu(s)$
9	$\lambda_{122}\lambda_{123}$	$\mu\tau$	$\tilde{\nu}_e(s+t)$	$\mu\tau$	$\tilde{\nu}_\mu(t)$
10	$\lambda_{122}\lambda_{131}$	$e\tau$	$\tilde{\nu}_e(s)$	—	—
11	$\lambda_{122}\lambda_{132}$	$\mu\tau$	$\tilde{\nu}_e(s+t)$	—	—
12	$\lambda_{122}\lambda_{133}$	$\tau\tau$	$\tilde{\nu}_e(s)$	—	—
13, 14, 15	$\lambda_{122}\lambda_{23k}$	—	—	—	—
16, 17, 18	$\lambda_{123}\lambda_{13k}$	—	—	—	—
19, 20, 21	$\lambda_{123}\lambda_{23k}$	—	—	—	—
22	$\lambda_{131}\lambda_{132}$	—	—	$e\mu$	$\tilde{\nu}_\tau(s+t)$
23	$\lambda_{131}\lambda_{133}$	—	—	$e\tau$	$\tilde{\nu}_\tau(s+t)$
24	$\lambda_{131}\lambda_{231}$	—	—	$e\mu$	$\tilde{\nu}_\tau(s)$
25	$\lambda_{131}\lambda_{232}$	ee	$\tilde{\nu}_\tau(s)$	$\mu\mu$	$\tilde{\nu}_\tau(s)$
26	$\lambda_{131}\lambda_{233}$	—	—	$\mu\tau$	$\tilde{\nu}_\tau(s)$
27	$\lambda_{132}\lambda_{133}$	—	—	$\mu\tau$	$\tilde{\nu}_\tau(t)$
28	$\lambda_{132}\lambda_{231}$	—	—	—	—
29	$\lambda_{132}\lambda_{232}$	$e\mu$	$\tilde{\nu}_\tau(s+t)$	—	—
30	$\lambda_{132}\lambda_{233}$	—	—	—	—
31	$\lambda_{133}\lambda_{231}$	—	—	—	—
32	$\lambda_{133}\lambda_{232}$	$e\tau$	$\tilde{\nu}_\tau(s)$	—	—
33	$\lambda_{133}\lambda_{233}$	—	—	—	—
34	$\lambda_{231}\lambda_{232}$	$e\mu$	$\tilde{\nu}_\tau(s+t)$	—	—
35	$\lambda_{231}\lambda_{233}$	$e\tau$	$\tilde{\nu}_\tau(t)$	—	—
36	$\lambda_{232}\lambda_{233}$	$\mu\tau$	$\tilde{\nu}_\tau(s+t)$	—	—

Table 4. Comparison between a $\mu^+\mu^-$ and an e^+e^- collider for processes leading to bounds on \mathbb{R}_p products of the $LL\bar{E}$ type. Dashes indicate inaccessibility, and $k = 1, 2, 3$ whenever it appears.

if muonic final states can be better identified, or at an e^+e^- collider if it is the electronic final states that can be better identified. One can also access different sneutrino resonances at the two types of machine, which may lead to different cross sections if the sneutrino masses are not degenerate.

For products of couplings, the graphs are very similar in the two cases, but applicable to different sets of products. We have noted that out of 36 products, only 12 can be accessed at a muon collider. Similarly 12 products can be accessed at an e^+e^- collider, with 4 products common to both. This leaves only 16 products that cannot be bounded when both machines run. This is illustrated in Table 4, where a full list of the products of λ -type couplings is shown, illustrating accessibility at both e^+e^- and $\mu^+\mu^-$ colliders.

We see, then, that a muon collider, with the same energy and luminosity parameters as an e^+e^- collider, can yield important new information about the nature of R -parity violation, especially in the case when the sfermion masses are large and low-energy bounds on the couplings are invalidated. With higher energies and luminosities, such as are planned for the NMC, one can obviously probe a larger region of parameter space. This provides at least one motivation for building such a machine.

7. Critique and Summary

Before concluding, it would be well to reiterate the weak points of the current analysis, which must be regarded as something of a zeroth-order study of the problem. In the first place, the work is futuristic, since nothing like a realistic design has been yet achieved for a muon collider, though intensive studies are under way. For this reason, energy and luminosity parameters are assumed to be those given by the Accelerator Physics Study Group at the Fermilab Workshop on the First Muon Collider [28]. These may change. It is also possible that the cuts on the angular distribution made in our analysis are too weak/strong and a future analysis can improve on it. The assumption of uniform detection efficiencies and the exact values assumed will probably change significantly, but though these will change the numerical results, none of our conclusions will change qualitatively. Finally, our study of final-state jets was done assuming that a jet forms a cone around the direction of the parent parton, and the thrust axis coincides with the parton momentum. This may change a little on inclusion of fragmentation effects, although cumulative experience with parton-level analyses suggests that such changes are small. However, a more detailed study might change the bin width and hence the number of bins, which is rather important for making the χ^2 analysis envisaged here. To sum up, numbers will change here and there for a variety of reasons, but we believe our general

conclusions to be fairly robust.

To summarize, then, we point out that the present constraints on some of the \mathcal{R}_p couplings are relatively weak. If the supersymmetric particles are light enough to be produced copiously at LEP, we shall shortly be in a position to witness dramatic signals. On the other hand, if they are either too heavy or too weakly coupled to be produced — as seems increasingly likely — indirect effects provide us with a means to investigate this sector. While a high-energy e^+e^- collider such as the NLC is obviously one facility where such searches can be carried out, we stress that a muon collider not only complements these results, but carries some of them further if high energies and luminosities can be attained. Quite a few of the lepton-number-violating \mathcal{R}_p couplings lead to significant deviations in the $\mu^+\mu^- \rightarrow f\bar{f}$ angular distributions. For some of the couplings, this effect can be used to impose bounds that are stronger than any available today, while for others it will provide a complementary test. This is particularly true if the sparticles turn out to have masses close to or above a TeV. A similar analysis would also be applicable to a large class of leptoquark and dilepton couplings. These results can, in fact, be mostly read-off from the ones presented in this article. Thus, it is clear that studies of R_p -violating supersymmetry and related models would benefit considerably from the construction of a muon collider.

Acknowledgements

The authors are grateful to the organizers of the Workshop on the First Muon Collider (Fermilab, 1997) for providing the motivation for this work. They would also like to thank S. Banerjee, J. Feng and N.K. Mondal for discussions. SR acknowledges partial financial support from the World Laboratory, Lausanne.

Appendix

Let us consider the process

$$\mu^-(p_1) + \mu^+(p_2) \rightarrow f(p_3) + \bar{f}(p_4) , \quad (10)$$

where f is a generic fermion of mass m_f . It is easy to ascertain that the most general amplitude for such a process can be expressed as

$$\begin{aligned} \mathcal{M} = & \sum_{a,b} \eta_{ab} \bar{u}(p_3) \gamma_\mu P_a v(p_4) \bar{v}(p_2) \gamma^\mu P_b u(p_1) + \sum_{a,b} \xi_{ab} \bar{u}(p_3) P_a v(p_4) \bar{v}(p_2) P_b u(p_1) \\ & + \omega \bar{u}(p_3) \sigma_{\mu\nu} v(p_4) \bar{v}(p_2) \sigma^{\mu\nu} u(p_1) \end{aligned} \quad (11)$$

where $a, b = L, R$ and $P_{L,R}$ are the chiral projection operators. The differential cross sections can then be expressed in terms of the Mandelstam variables s, t, u and the effective four-fermion coefficients η_{ab} , ξ_{ab} and ω . For the sake of simplicity, we choose to neglect the mass of the muon. On the other hand, we retain the effects of possible muon polarization. The latter can be parametrized as

$$\begin{aligned} a_{LL} &= (1 + \lambda_-)(1 + \lambda_+) & a_{LR} &= (1 - \lambda_-)(1 + \lambda_+) \\ a_{RL} &= (1 + \lambda_-)(1 - \lambda_+) & a_{RR} &= (1 - \lambda_-)(1 - \lambda_+) \end{aligned} \quad (12)$$

where λ_\pm give the degree of left polarization for μ^\pm . We have then

$$\begin{aligned} |\mathcal{M}|^2 = & \left[a_{LL} |\eta_{LL}|^2 + a_{RR} |\eta_{RR}|^2 \right] (u - m_f^2)^2 \\ & + \left[a_{LL} |\eta_{RL}|^2 + a_{RR} |\eta_{LR}|^2 \right] (t - m_f^2)^2 \\ & + 2m_f^2 s \left[a_{LL} \text{Re}(\eta_{LL} \eta_{RL}^*) + a_{RR} \text{Re}(\eta_{RR} \eta_{LR}^*) \right] \\ & + \frac{s^2}{4} \left[a_{LR} \left\{ |\xi_{RR}|^2 + |\xi_{LR}|^2 \right\} + a_{RL} \left\{ |\xi_{LL}|^2 + |\xi_{RL}|^2 \right\} \right] \\ & - \frac{m_f^2 s}{2} \left[a_{LR} |\xi_{RR} + \xi_{LR}|^2 + a_{RL} |\xi_{LL} + \xi_{RL}|^2 \right] \\ & + 8|\omega|^2 (1 - \lambda_+ \lambda_-) \left[(t - u)^2 + 2m_f^2 s \right] \\ & + 2s(u - t) \left[a_{LR} \text{Re}(\omega^* \xi_{RR}) + a_{RL} \text{Re}(\omega^* \xi_{LL}) \right] , \end{aligned} \quad (13)$$

and, finally,

$$\frac{d\sigma}{dt} = \frac{1}{16\pi s^2} |\mathcal{M}|^2 N_c \quad (14)$$

N_c being the appropriate colour factor.

The Standard Model expressions for η_{ab} and ξ_{ab} are obviously determined in terms of the fermion couplings to the neutral gauge bosons V_i ($\equiv \gamma/Z$). We choose to parametrize these as

$$\bar{f} \gamma^\mu \left(\ell_i^{(f)} P_L + r_i^{(f)} P_R \right) f V_i^\mu \quad (15)$$

with

$$\begin{aligned}
r_1^{(f)} &= eQ_f & \ell_1^{(f)} &= eQ_f \\
r_2^{(f)} &= \frac{e}{s_W c_W}(-s_W^2 Q_f) & \ell_1^{(f)} &= \frac{e}{s_W c_W}(T_{3f} - s_W^2 Q_f) .
\end{aligned} \tag{16}$$

With the above definitions, the SM expressions (for $f \neq \nu_\mu$) are given by

$$\begin{aligned}
\eta_{LL} &= \sum_i \left[\frac{\ell_i^{(\mu)} \ell_i^{(f)}}{s - M_i^2 + i\Gamma_i M_i} + \frac{(\ell_i^{(\mu)})^2}{t - M_i^2} \delta_{\mu f} \right] & \eta_{LR} &= \sum_i \frac{\ell_i^{(f)} r_i^{(\mu)}}{s - M_i^2 + i\Gamma_i M_i} \\
\eta_{RR} &= \sum_i \left[\frac{r_i^{(\mu)} r_i^{(f)}}{s - M_i^2 + i\Gamma_i M_i} + \frac{(r_i^{(\mu)})^2}{t - M_i^2} \delta_{\mu f} \right] & \eta_{RL} &= \sum_i \frac{r_i^{(f)} \ell_i^{(\mu)}}{s - M_i^2 + i\Gamma_i M_i} \\
\xi_{LL} &= 0 & \xi_{LR} &= -2 \sum_i \frac{\ell_i^{(\mu)} r_i^{(\mu)}}{t - M_i^2} \delta_{\mu f} \\
\xi_{RR} &= 0 & \xi_{RL} &= \xi_{LR} \\
\omega &= 0
\end{aligned} \tag{17}$$

In the presence of R_p -violating interactions, some of the four-fermion form-factors η_{ab} and ξ_{ab} will receive corrections (ω remains identically zero), with the form depending on the particular final state. The only non-zero corrections are:

$$\begin{aligned}
\mu^+ \mu^- \rightarrow \mu^+ \mu^- & : & \Delta\eta_{LR} = \Delta\eta_{RL} &= \sum_i \frac{\lambda_{i22}^2}{2(t - m_{\tilde{\nu}_i}^2)} \\
& & \Delta\xi_{LR} = \Delta\xi_{RL} &= -\sum_i \frac{\lambda_{i22}^2}{2(s - m_{\tilde{\nu}_i}^2 + i\Gamma_{\tilde{\nu}_i} m_{\tilde{\nu}_i})} \\
\mu^+ \mu^- \rightarrow e_k^+ e_k^- \quad (k \neq 2) & : & \Delta\eta_{LR} &= \sum_i \frac{\lambda_{ik2}^2}{2(t - m_{\tilde{\nu}_i}^2)} \\
& & \Delta\eta_{RL} &= \sum_i \frac{\lambda_{i2k}^2}{2(t - m_{\tilde{\nu}_i}^2)} \\
\mu^+ \mu^- \rightarrow d_k^+ d_k^- & : & \Delta\eta_{RL} &= \sum_i \frac{\lambda_{2ik}^{\prime 2}}{2(t - m_{\tilde{u}_{iL}}^2)}
\end{aligned} \tag{18}$$

References

- [1] For recent reviews, see, for example,
W. Hollik, Karlsruhe Univ. preprint KA-TP-22-1997 (1997), hep-ph/9711492;
G. Altarelli, CERN preprint CERN-TH-97-278 (1997), hep-ph/9710434.
- [2] H.P. Nilles, *Phys. Rep.* **110** (1984) 1;
H.E. Haber and G.L. Kane, *Phys. Rep.* **117** (1985) 75.
- [3] S. Weinberg, *Phys. Rev.* **26** (1982) 287;
N. Sakai and T. Yanagida, *Nucl. Phys.* **B197** (1982) 533;
C.S. Aulakh and R. Mohapatra, *Phys. Lett.* **B119** (1982) 136.
- [4] M.A. Diaz, Univ. of Valencia report no. IFIC-98-11 (1998), hep-ph/9802407, and references therein;
S. Roy and B. Mukhopadhyaya, *Phys. Rev.* **55** (1997) 7020.
- [5] G. Farrar and P. Fayet, *Phys. Lett.* **B76** (1978) 575.
- [6] F. Zwirner, *Phys. Lett.* **B132** (1983) 103;
J. Ellis *et al.*, *Phys. Lett.* **B150** (1985) 142;
G.G. Ross and J.W.F. Valle, *Phys. Lett.* **B151** (1985) 375;
S. Dawson, *Nucl. Phys.* **B261** (1985) 297;
S. Dimopoulos and L.J. Hall, *Phys. Lett.* **B207** (1987) 210.
L.J. Hall, *Mod. Phys. Lett.* **A5** (1990) 467.
- [7] L. J. Hall and M. Suzuki, *Nucl. Phys.* **B231** (1984) 419.
- [8] L.E. Ibañez and G.G. Ross, *Nucl. Phys.* **B368** (1992) 3.
- [9] A. Bouquet and P. Salati, *Nucl. Phys.* **B284** (1987) 557;
A.E. Nelson and S.M. Barr, *Phys. Lett.* **B246** (1990) 141;
B.A. Campbell *et al.*, *Phys. Lett.* **B256** (1991) 457;
W. Fischler *et al.*, *Phys. Lett.* **B258** (1991) 45.
- [10] H. Dreiner and G.G. Ross, *Nucl. Phys.* **B410** (1993) 188.
- [11] A.Yu. Smirnov and F. Vissani, *Phys. Lett.* **B380** (1996) 317;
K. Agashe and M. Graesser, *Phys. Rev.* **D54** (1996) 4445;
D. Choudhury and P. Roy, *Phys. Lett.* **B378** (1996) 153;
C.E. Carlson, P. Roy and M. Sher, *Phys. Lett.* **B357** (1995) 94.
- [12] V. Barger, G.F. Giudice and T. Han, *Phys. Rev.* **40** (1989) 2987.
- [13] G. Bhattacharyya and D. Choudhury, *Mod. Phys. Lett.* **A10** (1995) 1699.
- [14] R. Godbole, P. Roy and X. Tata, *Nucl. Phys.* **B401** (1993) 67.
- [15] M. Hirsch, H.V. Klapdor-Kleingrothaus and S.G. Kovalenko, *Phys. Rev. Lett.* **75** (1995) 17;
K.S. Babu and R.N. Mohapatra, *ibid.* **75** (1995) 2276.
- [16] G. Bhattacharyya, J. Ellis and K. Sridhar, *Mod. Phys. Lett.* **A10** (1995) 1583;
G. Bhattacharyya, D. Choudhury and K. Sridhar, *Phys. Lett.* **B355** (1995) 193.

- [17] H. Dreiner, in ‘Perspectives on Supersymmetry’, ed. G.L. Kane (World Scientific), hep-ph/9707435.
- [18] V. Barger, W.-Y. Keung and R.J.N. Phillips, *Phys. Lett.* **B364** (1995) 27; (E) *ibid.* **377** (1996) 486.
- [19] LEP2 workshop proceedings (chap. *Search for New Particles*) (CERN, 1995).
- [20] H. Baer, C. Kao and X. Tata, *Phys. Rev.* **D51** (1995) 2180 and references therein; M. Guchait and D.P. Roy, *Phys. Rev.* **D54** (1996) 3276; hep-ph/9707275.
- [21] D. Choudhury and S. Raychaudhuri, *Phys. Lett.* **B401** (1997) 54;
G. Altarelli *et al.*, *Nucl. Phys.* **B506**, (1997) 3;
H. Dreiner and P. Morawitz, *Nucl. Phys.* **B503**, (1997) 55;
J. Kalinowski, *et al. Z. Phys.* **C74** (1997) 595.
- [22] M. Drees, *Phys. Lett.* **B403**, (1997) 353.
- [23] D.K. Ghosh, R.M. Godbole and S. Raychaudhuri, in preparation.
- [24] H.-C. Cheng, Fermilab report no. FERMILAB-CONF-97-418-T (1997), hep-ph/9712427.
- [25] T. Kajita, Talk delivered on behalf of the Kamiokande and Super-Kamiokande Collaborations, Neutrino ’98, Japan (1998), <http://www-sk.icrr.u-tokyo.ac.jp/nu98/scan/063/>.
- [26] R.J. Oakes *et al.*, *Phys. Rev.* **57** (1998) 534;
A. Datta *et al.*, *Phys. Rev.* **56** (1997) 3107.
- [27] J.L. Feng, J.F. Gunion and T. Han, Madison report No. UCD-97-25 (1997), hep-ph/9711414.
- [28] See, for example, C. Ankenbrandt, Fermilab report No. FERMILAB-CONF-98-074 (1998), <http://www-lib.fnal.gov/archive/1998/conf/Conf-98-074.html>.
- [29] T. Aziz (L3 Collaboration), private communication.
- [30] Particle Data Group, *Phys. Rev.* **50** (1994) 1173.
- [31] R. Mohapatra, *Phys. Rev.* **34** (1986) 3457.